



## Correlation between tumor oxygenation and $^{18}\text{F}$ -fluoromisonidazole PET data simulated based on microvessel images

David Mönnich, Esther G. C. Troost, Johannes H. A. M. Kaanders, Wim J. G. Oyen, Markus Alber, Daniel Zips & Daniela Thorwarth

To cite this article: David Mönnich, Esther G. C. Troost, Johannes H. A. M. Kaanders, Wim J. G. Oyen, Markus Alber, Daniel Zips & Daniela Thorwarth (2013) Correlation between tumor oxygenation and  $^{18}\text{F}$ -fluoromisonidazole PET data simulated based on microvessel images, Acta Oncologica, 52:7, 1308-1313, DOI: [10.3109/0284186X.2013.812796](https://doi.org/10.3109/0284186X.2013.812796)

To link to this article: <https://doi.org/10.3109/0284186X.2013.812796>

 View supplementary material 

 Published online: 29 Aug 2013.

 Submit your article to this journal 

 Article views: 1088

 View related articles 

## ORIGINAL ARTICLE

**Correlation between tumor oxygenation and  $^{18}\text{F}$ -fluoromisonidazole PET data simulated based on microvessel images**DAVID MÖNNICH<sup>1</sup>, ESTHER G. C. TROOST<sup>2</sup>, JOHANNES H. A. M. KAANDERS<sup>3</sup>, WIM J. G. OYEN<sup>4</sup>, MARKUS ALBER<sup>5</sup>, DANIEL ZIPS<sup>6</sup> & DANIELA THORWARTH<sup>1</sup>

<sup>1</sup>Section for Biomedical Physics, Department of Radiation Oncology, University Hospital Tübingen, Tübingen, Germany, <sup>2</sup>Department of Radiation Oncology (MAASTRO), GROW School for Oncology and Developmental Biology, Maastricht University Medical Center, Maastricht, The Netherlands, <sup>3</sup>Institute of Oncology, Radiation Oncology, Radboud University Nijmegen Medical Centre, Nijmegen, The Netherlands, <sup>4</sup>Institute of Oncology, Nuclear Medicine, Radboud University Nijmegen Medical Centre, Nijmegen, The Netherlands, <sup>5</sup>Department of Radiation Oncology, Aarhus University, Aarhus, Denmark and <sup>6</sup>Department of Radiation Oncology, University Hospital Tübingen, Tübingen, Germany

**Abstract**

**Background.** Assessing hypoxia with oxygen probes provides a sparse sampling of tumor volumes only, bearing a risk of missing hypoxic regions. Full coverage is achieved with positron emission tomography (PET) using the tracer  $^{18}\text{F}$ -fluoromisonidazole (FMISO). In this study, the correlation between different FMISO PET imaging parameters and the median voxel  $\text{PO}_2$  (median $\text{PO}_2$ ) was analyzed. A measure of the median  $\text{PO}_2$  characterizes the microenvironment in consistency with probe measurements. **Material and methods.** Tissue oxygenations and FMISO diffusion-retention dynamics were simulated. Transport of FMISO and  $\text{O}_2$  molecules into and out of tissue was modeled by vessel maps derived from histology of head-and-neck squamous cell cancer xenograft tumor lines. Parameter sets were evaluated for 300 distinct  $2 \times 2 \text{ mm}^2$  vessel configurations, including median $\text{PO}_2$  and two FMISO PET parameters:  $F_{\text{H}}$  denotes the sub-regional signal four hours post injection (pi) and  $F_{\text{H/P}}$  denotes the ratio between  $F_{\text{H}}$  and the time-averaged signal 0–15 min pi. Correlations between  $\text{O}_2$  and FMISO parameters were evaluated. A receiver operating characteristics (ROC) analysis was performed, regarding the accuracy of  $F_{\text{H}}$  and  $F_{\text{H/P}}$  in identifying voxels with median $\text{PO}_2 < 2.5 \text{ mmHg}$ . **Results.** In hypoxic sub-regions, the correlation between  $F_{\text{H}}$  and median $\text{PO}_2$  is low ( $R^2 = 0.37$ ), while the correlation between  $F_{\text{H/P}}$  and median  $\text{PO}_2$  is high ( $R^2 = 0.99$ ). The ROC analysis showed that hypoxic regions can be identified using  $F_{\text{H/P}}$  with a higher diagnostic accuracy ( $\text{YI} = \text{sensitivity} + \text{specificity} - 1 = 1.0$ ), than using  $F_{\text{H}}$  alone ( $\text{YI} = 0.83$ ). Both FMISO parameters are moderately effective in identifying hypoxia on the microscopic length scale ( $\text{YI} = 0.63$  and  $0.60$ ). **Conclusions.** A combination of two FMISO PET scans acquired 0–15 min and four hours pi may yield an accurate measure of the median $\text{PO}_2$  in a voxel ( $F_{\text{H/P}}$ ). This measure is comparable to averaged oxygen probe measurements and has the advantage of covering the entire tumor volume. Therefore, it may improve the prediction of radiotherapy outcome and facilitate individualized dose prescriptions.

Radiotherapy (RT) is less effective in hypoxic tumors. Clinical studies have shown that therapy response correlates with tumor oxygen concentrations ( $\text{PO}_2$ ) measured with Eppendorf electrodes [1,2]. Oxygen probes yield an accurate measure of the local  $\text{PO}_2$  and the measurements are confined to a very small tissue volume [3]. However, they are invasive and limited to a few linear tracks across a tumor, i.e. it is impossible to assess the oxygenation in the entire tumor volume and as a consequence there is a risk

of missing severely hypoxic regions. These aspects may limit the applicability of probe measurements to derive a reliable overall prognosis of RT outcome and to guide the adaption of RT dose prescriptions to the local degrees of hypoxia-associated radioresistance (hypoxia dose painting [4,5]).

A three-dimensional assessment of tumor hypoxia is possible with positron emission tomography (PET) imaging using hypoxia tracers such as  $^{18}\text{F}$ -fluoromisonidazole (FMISO). Clinical studies have shown that

hypoxia PET imaging may be applicable to predict the overall RT response in different tumor entities including head-and-neck cancer [6–8]. However, direct voxel-based comparisons between hypoxia PET data and  $PO_2$  measurements using optical oxygen probes in preclinical tumor models were contradictory [9,10]. The authors hypothesized that a possible explanation is that oxygen probes assess the  $PO_2$  in vital and necrotic tissue alike, while FMISO accumulates in vital cells only. Therefore, in severely hypoxic voxels with a large amount of necrosis, the ambiguous situation may occur that a low average  $PO_2$  coincides with a very low tracer accumulation. Similar observations were made in clinical tumors by a study comparing FMISO PET and measurements with an Eppendorf electrode in different tumor entities [11].

This indicates that an assessment of the voxel-based  $PO_2$  by means of FMISO PET imaging with an accuracy comparable to that of probe measurements is intricate. It may require more comprehensive imaging protocols and dedicated tools for data analysis than an overall prognosis of RT outcome based on a single PET scan acquired several hours after tracer injection (pi).

The purpose of this study was to identify an FMISO PET imaging parameter that is an accurate measure of the median voxel  $PO_2$  as assessed by direct probe measurements. This parameter must overcome the limitations of imaging the FMISO accumulation at a single time point and may be useful to effectively guide hypoxia dose painting. In addition, its acquisition should be as simple as possible. Here, two parameters were considered that require either a single late PET scan (4 h pi) or the combination of a late scan and one immediately after tracer injection (0–15 minutes pi). The correlation between these parameters and the median of the underlying  $PO_2$  distribution was analyzed. The analysis was based on computational simulations of: 1) the tissue oxygenation; and subsequently, 2) the FMISO diffusion-accumulation dynamics for many different histology-derived microvessel arrangements [12].

## Material and methods

### *Tissue microsections and tumor microvessel maps*

In order to model the flux of  $O_2$  and FMISO molecules into and out of tissue in a biologically realistic manner, vessel maps were derived from tumor tissue histology. As described earlier [13], frozen tissue sections from human head-and-neck squamous cell cancer (SCCHN) xenograft tumor lines were immunohistochemically (IHC) stained for endothelial structures with 9F1 (rat monoclonal to mouse endothelium, Department of Pathology, Radboud University Nijmegen Medical Centre, Nijmegen,

The Netherlands). Subsequently, the sections were scanned using a digital image analysis system, resulting in gray-scale images of the fluorescent signal. In this study, five images from different tumors with a total area of 133 mm<sup>2</sup> were converted into vessel maps. The images were selected from a large database so that the vessel patterns varied strongly among as well as within the maps, ranging from very dense to sparse and inhomogeneous distributions. A total of 300 sub-regions with dimensions of  $2 \times 2$  mm<sup>2</sup> were placed in the maps at random locations. In these sub-regions, the studied  $O_2$  and FMISO parameters were calculated from the simulated data.

### *Modeling and simulation of $O_2$ and FMISO*

A tool to perform computer simulations of the FMISO diffusion-retention dynamics in multiple steps was used in this study. Its basic working principle is schematically shown in Supplementary Figure 1 available online at <http://informahealthcare.com/doi/abs/10.3109/0284186X.2013.812796>. The applied diffusion-reaction equations, simulation method and parameter values were described in detail earlier [12]. Briefly, equilibrium oxygen partial pressure ( $PO_2$ ) distributions are calculated for a given vessel map. The applied model accounts for the supply of oxygen across capillary membranes, its distribution in tissue and its consumption by tumor cells. A Michaelis-Menten relationship describes that cells decrease their oxygen consumption in line with a decreasing amount of available oxygen [14]. Subsequently, the  $PO_2$  distributions are used to calculate local FMISO binding rates. Binding rates are modeled to increase with decreasing  $PO_2$ , up to a sharp drop at very low  $PO_2$ . This drop accounts for cell death under extreme oxygen and glucose deprivation. In this way it is considered that FMISO is reduced in vital cells only. These assumptions agree qualitatively with Pimonidazole IHC in SCCHN xenografts [15]. Finally, by applying the  $PO_2$ -dependent local binding rates, FMISO supply, diffusion and retention are simulated in the same vessel map as the  $PO_2$ . By integrating the simulated FMISO concentrations in a specific sub-region, pseudo-PET voxel signals can be derived at different timepoints pi. Dividing these signals by the blood tracer concentration yields tumor-to-blood (T:B) ratios.

### *Simulated macroscopic $O_2$ and FMISO parameters*

In each sub-region the median oxygen partial pressure (median $PO_2$ ) was calculated. Two simulated FMISO parameters were calculated in each sub-region: 1) the mean FMISO concentration four hours pi,  $F_H = c(t = 4 \text{ h pi})$ ; and 2) the ratio between  $F_H$  and the average concentration 0–15 minute pi,  $F_{HP} = c(t = 4 \text{ h pi}) / \overline{c(t)}_{0-15\text{min}}$ . The second parameter

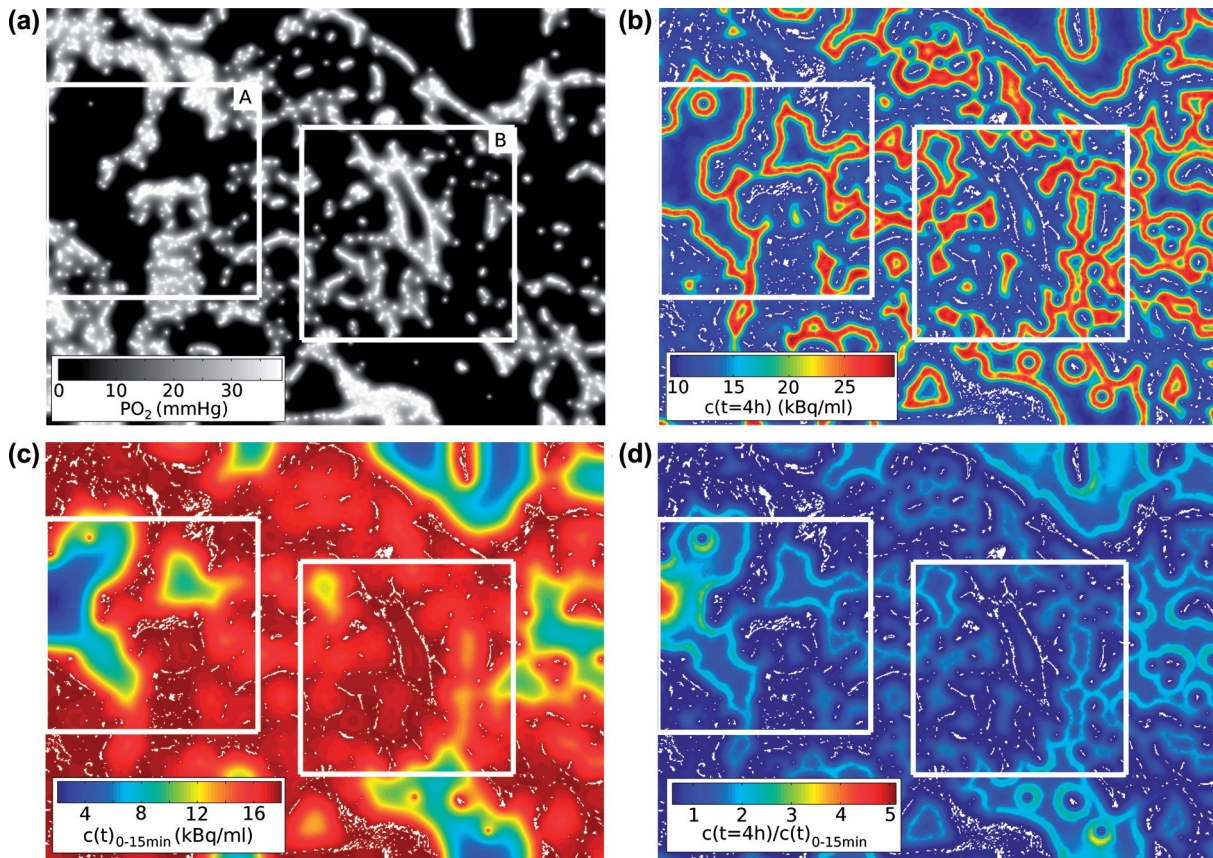


Figure 1. (a) Steady state  $\text{PO}_2$  distribution for a  $5.3 \times 3.9 \text{ mm}^2$  vessel map including two randomly placed  $2 \times 2 \text{ mm}^2$  sub-regions (A, B). (b) Corresponding distribution of FMISO 4 h pi. Sub-regional averaging yields  $F_H$ . Note the increasing retention with decreasing  $\text{PO}_2$  until it is diminished by necrosis. Vessels are white. (c) Averaged early FMISO signal. (d) Ratio between the distributions shown in (b) and (c) yields  $F_{H/P}$ . The median  $\text{PO}_2$  is substantially lower in sub-region A ( $9.4 \times 10^{-3} \text{ mmHg}$ ) than in B ( $7.1 \times 10^{-1} \text{ mmHg}$ ). Inconsistently,  $F_H$  is lower in A (15.0 kBq/ml) than in B (16.4 kBq/ml).  $F_{H/P}$  is higher in A (1.05) than in B (1.00) and thus is consistent with median  $\text{PO}_2$ .

can be interpreted as a measure of hypoxia-related tracer retention that is normalized by a simple measure of perfusion [16]. In this way, severely hypoxic regions containing much necrosis, in which small amounts of FMISO are retained, may nonetheless be correctly identified as having a low median  $\text{PO}_2$ , as they are typically poorly perfused as well.

#### Correlations between oxygenation and FMISO PET

Scatter plots of median  $\text{PO}_2$  against  $F_H$  as well as  $F_{H/P}$  were created. Furthermore, a correlation analysis was performed between median  $\text{PO}_2$  and the FMISO parameters. Coefficients of determination  $R^2$  were calculated in a linear sense (Pearson coefficient) and from non-linear fits.

Hypoxic sub-regions were segmented from all sub-regions by applying various thresholds to the simulated FMISO parameters. This emulates the method commonly used to identify hypoxia in FMISO PET images. In a receiver operating characteristic (ROC) analysis it was assessed how reliably sub-regions with a median  $\text{PO}_2$  below 2.5 mmHg can be identified when this

method is applied to  $F_H$  and  $F_{H/P}$ . In ROC curves, the true positive rate ( $\text{tpr} = \text{sensitivity}$ ) was plotted against the false positive rate ( $\text{fpr} = 1 - \text{specificity}$ ). The applied FMISO thresholds decrease along the curves. The area under the curves (AUC) and the Youden index ( $\text{YI} = \text{tpr} - \text{fpr}$ ) were calculated as quality measures. Their values may range from 0.5 to 1 and 0 to 1 (no predictive value to strong predictive value), respectively. In a further step, the ROC analysis was also used to evaluate how well the FMISO parameters characterize the micro  $\text{PO}_2$  values on the cellular level. In this case, each parameter represents a  $60 \times 60$  matrix of underlying  $\text{PO}_2$  values.

## Results

#### Simulated oxygenations

Full simulations were performed for the five vessel maps. An example for a simulated equilibrium  $\text{PO}_2$  distribution and the corresponding static FMISO micropattern four hours pi is shown in Figure 1a. The median micro  $\text{PO}_2$  value of all maps was 10.0 mmHg and ranged from 0.0 mmHg to 40.0 mmHg. The micro  $\text{PO}_2$  was calculated with a spatial resolution of

50  $\mu\text{m}/\text{pixel}$ , which is comparable to Eppendorf electrodes [3]. Histograms of the micro $\text{PO}_2$  within four selected sub-regions show distinct oxygenation patterns (Supplementary Figure 2 available online at <http://informahealthcare.com/doi/abs/10.3109/0284186X.2013.812796>). The simulated sub-regional median $\text{PO}_2$  ranged from  $8 \times 10^{-3}$  mmHg to 33.8 mmHg with a median of 7.0 mmHg.

#### Correlations between oxygenation and FMISO PET

In Figure 2a a scatter plot of median $\text{PO}_2$  against  $F_H$  is shown. Each point represents a data pair from a specific sub-region. A high overall linear correlation coefficient  $R^2$  of 0.95 was observed. This value reduces to 0.37 when the analysis is restricted to data pairs in the hypoxic range (i.e. median $\text{PO}_2 < 10$  mmHg). However, a high accuracy is especially important in this range. In Figure 1 it is demonstrated for two selected sub-regions that the low FMISO retention in regions with a large amount of necrosis is an important reason for the low correlation between  $F_H$  and median $\text{PO}_2$  in hypoxic tissue.

A plot of the median $\text{PO}_2$  against the perfusion-normalized FMISO parameter  $F_{H/P}$  is shown in Figure 2b. By visual inspection a well-defined non-linear relationship was found, especially in the hypoxic range. This was corroborated by fitting the function  $f(x) = p_1/(p_2 + x)^{p_3} + p_4$  to the data. The resulting fit coefficients were  $[p_1, p_2, p_3, p_4] = [568 \text{ mmHg}, 0.575, 10.0, -0.210 \text{ mmHg}]$ . A coefficient of determination  $R^2$  between median $\text{PO}_2$  and  $F_{H/P}$  of 0.98 was found for the overall data and of 0.99 for the data in the hypoxic range. This suggests that  $F_{H/P}$  is a more accurate measure of the median $\text{PO}_2$  than  $F_H$ .

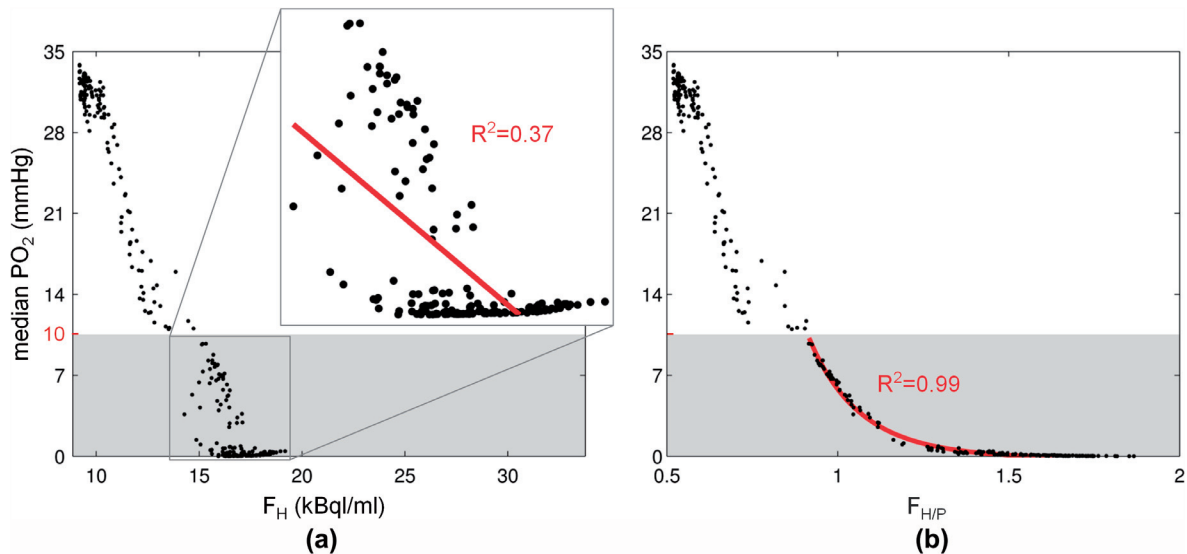


Figure 2. Scatter plots of median $\text{PO}_2$  against (a)  $F_H$  and (b)  $F_{H/P}$ . Red lines are fits restricted to hypoxic sub-regions (median $\text{PO}_2 < 10$  mmHg). Coefficients of determination  $R^2$  for the restricted fits indicate a low correlation between median $\text{PO}_2$  and  $F_H$  and a high correlation between median $\text{PO}_2$  and  $F_{H/P}$ .

#### ROC analysis

The ROC analysis of the diagnostic accuracies of the simulated FMISO parameters to identify hypoxia is shown in Figure 3. Clearly, sub-regions with a critical median $\text{PO}_2$  below 2.5 mmHg are discriminated extremely well by  $F_{H/P}$  (AUC = 1.0, optimum YI = tpr-fpr = 1.0), while  $F_H$  alone is less reliable (AUC = 0.97, YI = 0.83). The optimum threshold values were  $F_{H/P} = 1.1$  and  $F_H = 16.1$  kBq/ml (T:B = 1.8).

The ROC analysis with regard to the identification of microscopic hypoxia (micro $\text{PO}_2$ ) based on the macroscopic FMISO parameters gave a slightly different picture. It resulted in AUC (optimum YI) of 0.88 (0.63) and 0.86 (0.60) for  $F_{H/P}$  and  $F_H$ , respectively. These values are considerably lower than for the identification of sub-regions with a critical macroscopic median $\text{PO}_2$  based on either of the FMISO parameters. Here, the optimum threshold values were  $F_{H/P} = 1.0$  and  $F_H = 15.5$  kBq/ml (T:B = 1.7).

#### Discussion

The results of this study outline how the fundamental limitations of FMISO PET imaging affect its value as a measure of the  $\text{PO}_2$  in a voxel. The first limitation is that a macroscopic imaging modality is used to image hypoxia, which is a microscopic phenomenon. Therefore, the measured signal is an average over a very heterogeneous distribution of hypoxia levels on the microscopic length scale. Another important aspect is the ambiguous binding behavior of the FMISO molecule: it shows a low accumulation in severely hypoxic regions containing a large amount of necrosis. As a consequence, these regions cannot be distinguished

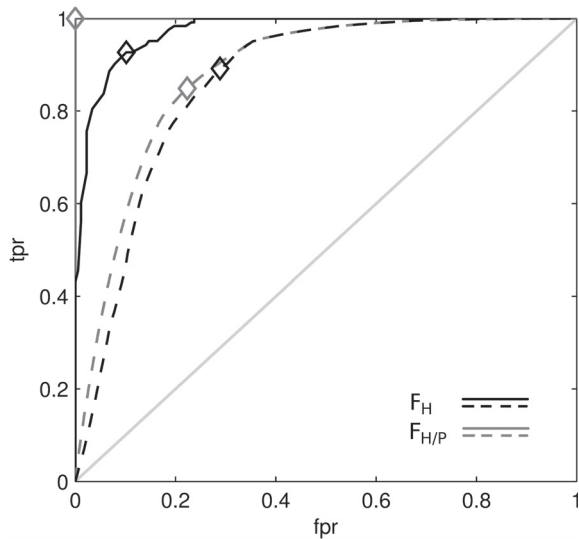


Figure 3. Receiver operating characteristic of  $F_{H/P}$  (gray curves) and  $F_H$  (black curves) for the identification of hypoxia. Solid lines refer to the identification of a median $PO_2 < 2.5$  mmHg in macroscopic sub-regions. Dashed lines refer to the identification of micro $PO_2 < 2.5$  mmHg in the  $60 \times 60$   $PO_2$  values underlying each FMISO parameter. Cut-off values applied to the FMISO parameters decrease along the curves from left to right. Optimum points are marked. The identification of critical median $PO_2$  is very sensitive and specific using  $F_{H/P}$  (optimum YI = 1.0). Using  $F_H$  is less effective (YI = 0.83). Both parameters are moderately accurate in identifying critical micro $PO_2$  values (YI = 0.63 and 0.60).

from well-oxygenated regions in FMISO PET images acquired during the tracer uptake phase. These limitations have also been observed in preclinical tumor models using  $^{18}F$ -Fluoroazomycin Arabinoside (FAZA) autoradiography and Pimonidazole IHC [17].

Here, a method was proposed to compensate the deficient tracer accumulation due to necrosis by incorporating supplementary information. For this purpose, the simulated PET signal during the FMISO wash-in phase (0–15 minute pi) was used, as it characterizes the vessel network in a voxel and therefore identifies poorly perfused voxels independently of the FMISO accumulation (cf. Figure 1c). The results show, that the proposed combined parameter  $F_{H/P}$  is a much more accurate measure of the median $PO_2$  than the uptake parameter  $F_H$  alone. This indicates that  $F_{H/P}$  characterizes the tissue microenvironment in a similar manner as measurements with oxygen probes. However, FMISO PET imaging overcomes the limitation of oxygen probes of sampling the  $PO_2$  in small parts of a tumor only. These results corroborate a preclinical study correlating optical oxygen probe measurements with FMISO PET imaging, in which severely hypoxic voxels with low  $PO_2$  readings presented low FMISO intensities two hours pi [9].

The large range of oxygenation levels that are averaged in a PET voxel signal cannot be recovered. This is demonstrated by the relatively low diagnostic

accuracy of  $F_H$  as well as  $F_{H/P}$  with respect to the identification of micro $PO_2$  values below 2.5 mmHg. The accuracies simulated in this work are comparable to results from a preclinical study analyzing FMISO PET signals and oxygen probe readings on a voxel-by-voxel basis [10]. A moderate accuracy was reported for the identification of micro $PO_2$  values below 2.5 mmHg using the two hour pi equivalent to  $F_H$  acquired with a sub-millimeter resolution. As fully dynamic FMISO PET was performed in this study, the method offers a potential to validate the theoretical results of the present work.

Quantitative aspects of the results must be interpreted with great care. In a clinical setting, the correlations and diagnostic accuracies presumably are substantially lower than estimated here. There are a number of reasons for this. For instance, the achievable resolution in clinical PET imaging is lower than the edge length of 2 mm of the simulated sub-regions. Inter-patient variations of the tracer pharmacokinetics, such as tracer clearance and metabolite forming, also have an influence. Furthermore, image noise was not included in the analysis and simulations were performed in 2D. Though, as these factors influence  $F_H$  and  $F_{H/P}$  alike, the general conclusion holds that the perfusion-normalized uptake parameter  $F_{H/P}$  is a more accurate measure of the median $PO_2$  than the uptake parameter  $F_H$  alone.

The early acquisition interval of 0–15 minutes has not been varied in this study. It is well possible that a shorter scan provides identical information. The length and position of the interval can be optimized in a preclinical validation study combining spatially co-registered dynamical FMISO PET and oxygen probe measurements, which is technologically feasible [10]. A validation of the presented results is moreover needed, because not every biological effect can be accounted for by the simulation model. For example, the proposed parameter  $F_{H/P}$  may be less accurate when tissue perfusion and hypoxia levels are uncoupled. This situation may arise in tissue regions that are dominated by hemoglobin deficient plasma flow. Such regions can be very hypoxic (high FMISO retention) and at the same time well perfused (high wash-in signal).

Incorporating the wash-in phase FMISO PET signal does not only allow to compensate the low tracer accumulation in severely hypoxic voxels, it may also yield a prediction of the development of the hypoxic microenvironment during RT, e.g. the reoxygenation potential of a tissue region [18]. This could explain why clinical results indicate that optimum timepoints for isolated uptake imaging might lie weeks into the course of therapy [6,19]. In contrast, a full kinetic analysis of dynamic FMISO PET data allows the estimation of treatment outcome prior to the initiation of

RT [16]. The parameter  $F_{HP}$  proposed here was designed to capture the essential information of dynamic FMISO PET imaging, i.e. the independent information from the tracer wash-in as well as the uptake phase, yet avoiding the complex acquisition and analysis of fully dynamic data. However, potential issues arising from patient repositioning between the two PET scans and subsequent image co-registration remain. Should this compromise the usefulness of the proposed method, moving the patient off the table between scans may be avoided by obtaining a perfusion measure from a  $^{15}\text{O}$ -Water PET scan or a suitable MRI or DCE CT protocol in a combined scanner.

## Conclusions

In this study, tissue oxygenations and FMISO diffusion-retention dynamics were computationally simulated. The correlation between simulated partial oxygen pressures and different FMISO PET parameters was analyzed. The results show that the median  $\text{PO}_2$  in a PET voxel can be assessed with high accuracy by combining independent information from early (0–15 minutes pi) and late (four hours pi) FMISO PET scans. Using a late scan only is less accurate. Both methods recover the oxygenation on the cellular level with moderate accuracy.

**Declaration of interest:** The authors report no conflicts of interest. The authors alone are responsible for the content and writing of the paper.

This project was financially supported by the German Research Foundation (DFG), grant no. TH 1528/1-1 and by the European Social Fund and the Ministry of Science, Research and the Arts Baden-Württemberg.

## References

- [1] Höckel M, Schienger K, Aral B, Milze M, Schäffer U, Vaupel P. Association between tumor hypoxia and malignant progression in advanced cancer of the uterine cervix. *Cancer Res* 1996;56:4509–15.
- [2] Nordmark M, Bentzen SM, Rudat V, Brizel D, Lartigau E, Stadler P, et al. Prognostic value of tumor oxygenation in 397 head and neck tumors after primary radiation therapy. An international multi-center study. *Radiother Oncol* 2005;77:18–24.
- [3] Griffiths JR, Robinson SP. The OxyLite: A fibre-optic oxygen sensor. *Br J Radiol* 1999;72:627–30.
- [4] Thorwarth D, Eschmann SM, Paulsen F, Alber M. Hypoxia dose painting by numbers: A planning study. *Int J Radiat Oncol Biol Phys* 2007;68:291–300.
- [5] Toma-Daşa I, Uhrdin J, Antonovic L, Da u A, Nuyts S, Dirix P, et al. Dose prescription and treatment planning based on FMISO-PET hypoxia. *Acta Oncol* 2012;51:222–30.
- [6] Zips D, Zöphel K, Abolmaali N, Perrin R, Abramyuk A, Haase R, et al. Exploratory prospective trial of hypoxia-specific PET imaging during radiochemotherapy in patients with locally advanced head-and-neck cancer. *Radiother Oncol* 2012;105:21–8.
- [7] Mortensen LS, Johansen J, Kallehauge J, Primdahl H, Busk M, Lassen P, et al. FAZA PET/CT hypoxia imaging in patients with squamous cell carcinoma of the head and neck treated with radiotherapy: Results from the DAHANCA 24 trial. *Radiother Oncol* 2012;105:14–20.
- [8] Horsman MR, Mortensen LS, Petersen JB, Busk M, Overgaard J. Imaging hypoxia to improve radiotherapy outcome. *Nat Rev Clin Oncol* 2012;9:674–87.
- [9] Chang J, Wen B, Kazanzides P, Zanzonico P, Finn RD, Fichtinger G, et al. A robotic system for [18F]-FMISO PET-guided intratumoral pO<sub>2</sub> measurements. *Med Phys* 2009;36:5301–9.
- [10] Bartlett RM, Beattie BJ, Naryanan M, Georgi J-C, Chen Q, Carlin SD, et al. Image-guided Po<sub>2</sub> probe measurements correlated with parametric images derived from 18F-fluoromisonidazole small-animal PET data in rats. *J Nucl Med* 2012;53:1608–15.
- [11] Mortensen LS, Buus S, Nordmark M, Bentzen L, Munk OL, Keiding S, et al. Identifying hypoxia in human tumors: A correlation study between 18F-FMISO PET and the Eppendorf oxygen-sensitive electrode. *Acta Oncol* 2010;49:934–40.
- [12] Mönnich D, Troost EGC, Kaanders JHAM, Oyen WJG, Alber M, Thorwarth D. Modelling and simulation of [18F] fluoromisonidazole dynamics based on histology-derived microvessel maps. *Phys Med Biol* 2011;56:2045–57.
- [13] Bussink J, Kaanders JHAM, Rijken PFJW, Raleigh JA, Van der Kogel AJ. Changes in blood perfusion and hypoxia after irradiation of a human squamous cell carcinoma xenograft tumor line. *Radiat Res* 2000;153:398–404.
- [14] Casciari JJ, Sotirchos SV, Sutherland RM. Variations in tumor cell growth rates and metabolism with oxygen concentration, glucose concentration, and extracellular pH. *J Cell Physiol* 1992;151:386–94.
- [15] Ljungkvist ASE, Bussink J, Kaanders JHAM, Rijken PFJW, Begg AC, Raleigh JA, et al. Hypoxic cell turnover in different solid tumor lines. *Int J Radiat Oncol Biol Phys* 2005;62:1157–68.
- [16] Thorwarth D, Eschmann S-M, Scheiderbauer J, Paulsen F, Alber M. Kinetic analysis of dynamic 18F-fluoromisonidazole PET correlates with radiation treatment outcome in head-and-neck cancer. *BMC Cancer* 2005;5:152.
- [17] Busk M, Horsman MR, Overgaard J. Resolution in PET hypoxia imaging: Voxel size matters. *Acta Oncol* 2008;47:1201–10.
- [18] Thorwarth D, Eschmann S-M, Paulsen F, Alber M. A model of reoxygenation dynamics of head-and-neck tumors based on serial 18F-fluoromisonidazole positron emission tomography investigations. *Int J Radiat Oncol Biol Phys* 2007;68:515–21.
- [19] Eschmann SM, Paulsen F, Bedeshem C, Machulla H-J, Hehr T, Bamberg M, et al. Hypoxia-imaging with 18F-Misonidazole and PET: Changes of kinetics during radiotherapy of head-and-neck cancer. *Radiother Oncol* 2007;83:406–10.

## Supplementary material available online

Supplementary Figures 1–2